

A Study on Increasing of Heat Flux for Heat Sink in VRF Outdoor Inverter Board

Hoai-An Le¹, Minh-Hung Doan^{2*}

Ho Chi Minh City University of Technology and Education, Vietnam

*Corresponding author. Email: hungdm@hcmute.edu.vn

ARTICLE INFO

Received: 08/06/2024
Revised: 05/07/2024
Accepted: 19/07/2024
Published: 28/02/2025

KEYWORDS

Mini-channel heat sink;
VRF outdoor inverter board;
Heat flux;
Heat sink performance;
Heat exchanger area.

ABSTRACT

Increasing of heat flux for heat sink in VRF outdoor inverter board helps to increase heat sink performance, prevent over heat error caused by inverter board. For these reasons, the heat sinks are carried out to experimentally study, propose an R22 air conditioner model with the heat sinks in conditions of different hydraulic diameter (D_h), copper tube quantity (n). Three samples are same length L (150 mm), W (140 mm), HS1 sample has D_h (10.7 mm), n (1 tube); HS2 sample has D_h (4.35 mm), n (6 tubes); HS3 sample has D_h (2.98mm), n (9 tubes). While increasing resistor capacity from 100 W to 450 W, the surface temperature (chip) increases from 65°C to 105°C, leads the temperature difference of refrigerant fluid also increases. While the chip temperature obtains 105 °C, the maximum temperature difference of refrigerant fluid of HS2 (4.9°C) is higher 6.5%, 19.5% if compared to HS1 (4.6°C), HS2 (4.1°C), respectively. Besides, while increasing resistor capacity, heat flux increases. At 400 W, heat flux of HS1, HS2, HS3 obtains 20047 W/m², 19294 W/m², 17712 W/m², respectively. Results show the heat flux of HS2 is respectively higher 4%, 13% if compared to HS1, HS3. Result shows that heat transfer coefficient of HS2 is higher 7%, 18% if compared to HS1, HS3. The results show that increasing of heat exchanger performance. It can be completely applied to VRF outdoor system to help to reduce over heat error in VRF outdoor inverter board. This study will serve as the basis of increasing of heat flux and is the foundation for improving heat sinks.

Doi: <https://doi.org/10.54644/jte.2025.1612>

Copyright © JTE. This is an open access article distributed under the terms and conditions of the [Creative Commons Attribution-NonCommercial 4.0 International License](https://creativecommons.org/licenses/by-nc/4.0/) which permits unrestricted use, distribution, and reproduction in any medium for non-commercial purpose, provided the original work is properly cited.

1. Introduction

Engineering fields in general and thermal engineering technology in particular are playing an important role in the application of mini-channel heat exchangers in many fields of science and technology today. Research directions in this field play an important role for mini-channel heat transfer technology. Based on an overview of research works, it has been shown that the heat transfer process in a heat sink which depends on many factors such as: size, length, type of fluid used, temperature and flow of the fluid. A study on five different channel shapes using a novel scheme for meshing and a structure of a multi-nozzle microchannel heat sink which performed by Tran et al [1] thru a copper plate measuring 9.8 mm x 9.8 mm x 0.5 mm was used as a fixed substrate for designs with single-layer-and-parallel or multi-nozzle microchannel heat sinks. Nascimento et al [2] did an experimental study on flow boiling heat transfer of R134a in a microchannel-based heat sink. Thiangtham et al [3] did an experimental study on two-phase flow patterns and heat transfer characteristics during boiling of R134a flowing through a multi microchannel heat sink. Karwa et al [4] tested using CFD simulations and experimentally using a 3D printed prototype on development of a low thermal resistance water jet cooled heat sink for thermoelectric refrigerators to increase the performance of thermoelectric coolers, to reduce the thermal resistances of the heat sinks. Wang et al [5] did a study on effecting of the number of circuits on a finned-tube heat exchanger performance and its improvement by a reversely variable circuitry. Xia et al [6] did a study on effects of different geometric structures on fluid flow and heat transfer performance in microchannel heat sink by numerical investigation. Madhour et al [7] studied flow

boiling of R134a in a multi-microchannel heat sink with hotspot heaters for energy-efficient microelectronic CPU cooling applications. Mohammed et al [8] studied on influence of channel shape on the thermal and hydraulic performance of microchannel heat sink by numerical simulations. Vafai et al [9] did analysis of two-layered micro-channel heat sink concept in electronic cooling. Khan et al [10] did investigation of heat transfer and pressure drop in microchannel heat sink using Al₂O₃ and ZrO₂ nanofluids.

As above mentioned reviews, previous authors studied on the heat sinks using fluid by R134a refrigerant and water, the heat sinks using fluid by nanofluids and water, the heat sinks using fluid by R134a, R235fa, R245fa and water. Research on improving heat flux for heat sinks on VRF outdoor inverter board has not been fully published and detailed. Therefore, the study on "A study on increasing of heat flux for heat sink in VRF outdoor inverter board" is necessary.

To summarize, it is essential to carry out an in-dept study on increasing of heat flux for heat sink in VRF outdoor inverter board in order to help improve their design and optimize their performance. Three samples for HS1, HS2, and HS3 were investigated. In the following sections, two cases will be discussed: (1) the mass flow rate and inlet temperature are constant for refrigerant (2) the heater temperature are variable for the thermal resistance. In details, experimental study with three samples: With HS1 sample, respective length, width, thickness, hydraulic diameter size and copper tube quantity of HS1 sample are 150 mm, 140 mm, 32 mm, and $D_h = 10.7$ mm, $n = 1$. With HS2 sample, respective length, width, thickness, hydraulic diameter size and copper tube quantity of HS2 sample are 150 mm, 140 mm, 22 mm, and $D_h = 4.35$ mm, $n = 6$. With HS3 sample, respective length, width, thickness, hydraulic diameter size, and copper tube quantity of HS3 sample are 150 mm, 140 mm, 22 mm, and $D_h = 2.98$ mm, $n = 9$.

Nomenclature:	t_f - mean temperature of atmosphere, °C
c_p - specific heat, kJ/(kgK)	t_k - condenser temperature, °C
D_h - hydraulic diameter, m	t_{ht} - resistance heater temperature, °C
F - area, m ²	t_o - evaporator temperature, °C
k - heat transfer coefficient, kW/(m ² K)	t_w - surface mean temperature of heat sink, °C
L - length, mm	W - width, mm
m - mass flow rate, kg/s	Greek symbols:
p_1 - pressure at the inlet, (Pa)	α - heat transfer coefficient, kW/(m ² K)
p_2 - pressure at the outlet, (Pa)	Δp - pressure drop of heat sink, Pa
q - heat flux, kW/m ²	Δt - different temperature of fluid, °C
Q - heat transfer rate, kW	Δt_{LMTD} - logarithmic mean temperature difference, °C
T - thickness, mm	δ - the plate thickness, m
T_a - ambient temperature, K	λ - thermal conductivity, W/(mK)
t_{chip} - surface temperature of chip, °C	

2. Experimental method

2.1. Setting up the experimental system

In this experimental system, two main parts are used: the experimental sample (heat sink) and the heater (thermal resistance), air conditioning system is using R22, completes with copper tube system, as shown in Fig. 1. In this study, a heat sink is used for investigation. The heater by thermal resistance and the heat sink are installed so that both of them can closely contact between two surfaces. The heat transfer process of these devices is carried out between the heat sink and the heater. Four sensors are installed in middle of the heat sink and the heater. Fig. 2 shows the experimental sample dimension. Aluminum is used for making this heat sink, with thermal conductivity is 237 W/(mK), specific mass is 2700 kg/m³ and specific heat at constant pressure is 904 J/(kgK).

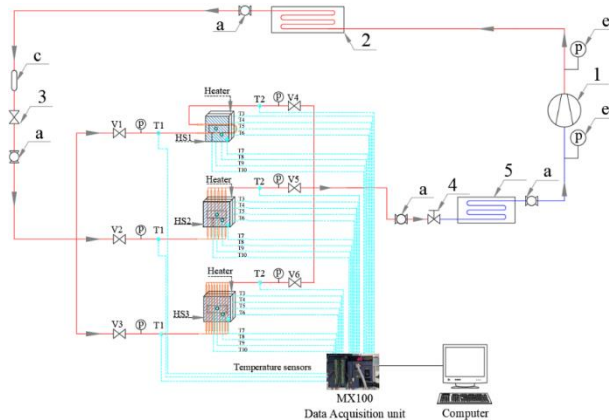


Fig. 1. Experimental system diagram



Fig. 2. The experimental system photo

Where: HS1 - Heat sink 1, HS2 - Heat sink 2, HS3 - Heat sink 3, 1 - Compressor, 2 - Condenser, 3 - Gate valve, 4 - Expansion valve, 5 - Evaporator, a - Gas glass, c - Filter, e - Pressure gauge, V1, V2, V3, V4, V5, V6 - Gate valve, T10 - Temperature sensor of heater, T1- Inlet refrigerant temperature sensor, T2- Outlet refrigerant temperature sensor, T3, T4, T5, T6 - Inner surface (chip) temperature sensor of heat sink, T7, T8, T9 - Outside surface temperature sensor of heat sink.

With this cycle, in case of experimenting on heat sink HS1, gate valves V1, V2, V3 open, gate valve V4 opens, and V5, V6 close. While experimenting on heat sink HS2, gate valves V1, V2, V3 open, gate valve V5 opens, and V4, V6 close. While experimenting on heat sink HS3, gate valves V1, V2, V3 open, gate valve V6 opens, and V4, V5 close. At heat sink, temperature parameters on heat sink surface will be measured by MX100 temperature measuring equipment. In this experimental model, will use emulator heat by heater to replace for the heat source which creates from outdoor unit board to create corresponding heat source for heat sink in this experimental condition.

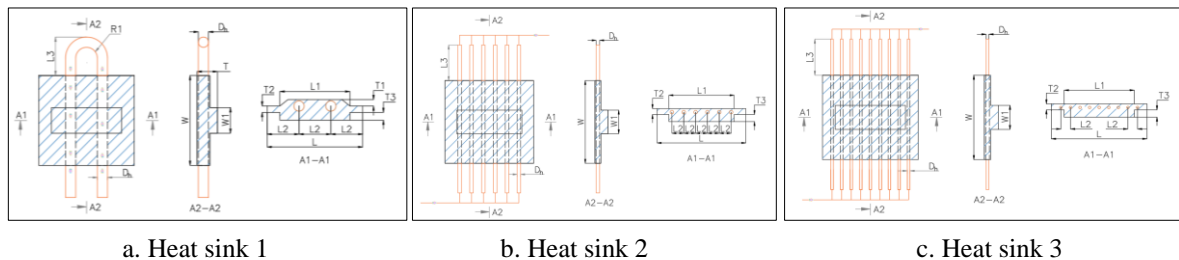


Fig. 3. Experimental sample dimensions

Fig. 3 describes dimensions of 3 experimental samples. In this study, heat sink is designed and made based on actual system with dimensions in Table 1. Fig. 4 shows photos of heat sinks. These test sections were manufactured by computerized numerical control machining (CNC).

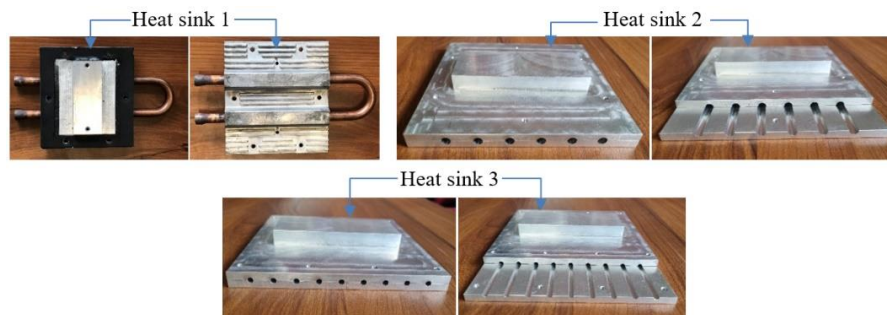


Fig. 4. Photos of heat sinks

Fig. 5 show photos of a heat sink using aluminum materials. This sample is endeavour as actual system air conditioning. Front section area is 21000 mm² (W x L). Behind section area is 8800 mm²

($W_1 \times L_1$) will closely contact to heater. Heat sink and heater insulated by PE insulation material as Fig. 6. Insulation physical properties in Table 2.

Table 1. Geometric parameters of heat sink

Sample	Heat sink dimension (mm)				Detailed dimension (mm)						
	L	W	T	W_1	L_1	L_2	L_3	T1	T2	T3	Dh
HS1	150	140	32	40	110	50	60	10	10	12	10.7
HS2	150	140	22	40	110	20	60	-	10	12	4.35
HS3	150	140	22	40	110	15	60	-	10	12	2.98

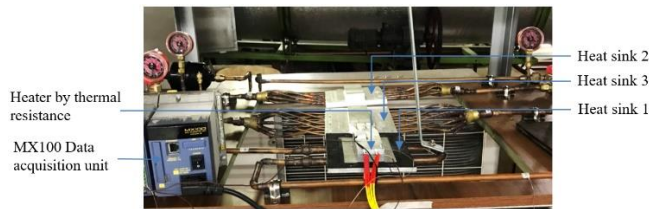


Fig. 5. Heat sinks location

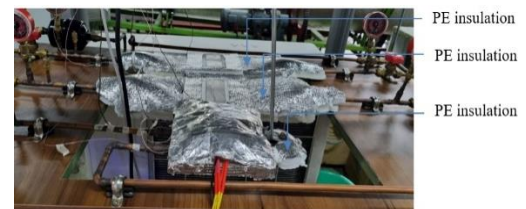


Fig. 6. PE insulation material

Table 2. Insulation physical properties

Material	Specific mass (kg/m^3)	Thermal conductivity $W/(mK)$
PE insulation	25	0.032

The experimental system photos show in Fig. 2. The experimental data obtained from the heat sinks were under room temperature condition at 33 °C. Gas R22 used as working liquid. Every inlet and outlet of heat sink was installed two sensors and pressure gauges in order to measure temperature and pressure parameter. Other temperature sensors were located as shown in Fig. 7. Where T1 is inlet refrigerant temperature sensor, T2 is outlet refrigerant temperature sensor, T3 to T6 are inner surface (chip) temperature sensor of heat sink, T7 to T9 are outside surface temperature sensor of heat sink and T10 is temperature sensor of heater, T11 is ambient temperature sensor

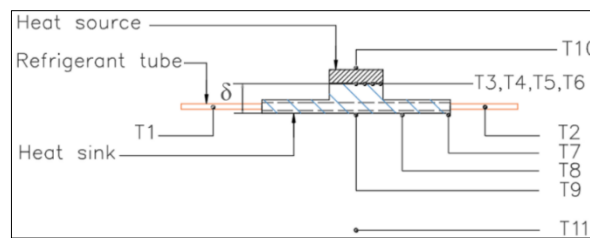


Fig. 7. The locations of temperature sensors on the heat sink

In addition, thermal camera was used to able to scan the surface temperature of the heat sinks. Equipments used for the experiments are listed in Table 3. Accuracies and ranges of testing apparatuses are listed in Table 4.

Table 3. Equipments used for the experiments

No	Equipment	Model	Origin
1	Data acquisition unit	MX100	Japan
2	Digital clamp meter	52240 Mastercool	USA
3	Gas charge gauge	94261 Mastercool	USA

4	Temperature measuring device	52224-A Mastercool	USA
5	Gas charge valve	90328 Mastercool	USA
6	Pressure gauge	94261 Mastercool	USA
7	Air conditioner	AC036HCBDGD/EA	Samsung
8	Heat sink	HS1/HS2, HS3	Samsung/Viet Nam
9	Dimmer kit	HP5J	China
10	Thermal camera	UTi220B	China
11	Thermal resistance		Viet Nam

Table 4. *Accuracies and ranges of testing apparatuses*

Testing apparatus	Accuracy	Range
Thermocouple	$\pm 0.01\%$	-200 to 400 °C
Pressure gauge	$\pm 0.5\%$ FS	-14.5 to 800 psi
Temperature gauge	± 0.1 °C	-50 to 70 °C
Thermal camera	$\pm 2\%$	-20 to 550 °C
Digital clamp meter	$\pm 2\%$ A, $\pm 1.2\%$ V	0 to 600 A, 0 to 750 V

Before measuring temperature, all sensors displayed same value. Next step, the experimental system was maintained to let be settled operation about 30 minutes then started to get parameters. Then, temperature value was recorded and calculated by average temperature of sensors. Similarly, pressure value was recorded.

2.2. Experimental method

In order to study to increase heat flux for the heat sink, experimental conditions for the heat sink were kept. In this study, three experimental cases are discussed: three cases kept the inlet refrigerant temperature of the heat sinks and variable temperature of the heater thru thermal resistance. The experimental studies are detailed as follows: (1) Experiment 1: Applying to $D_h = 10.7$ mm, tube quantity $n = 1$ (Heat sink HS1) in case of keeping the inlet refrigerant temperature of heat sink. Constant liquid temperature ($t_k = 45$ °C), the chip temperature ($t_{chip} = \text{variable}$) within 65 °C to 105 °C. (2) Experiment 2: Applying to $D_h = 4.35$ mm, tube quantity $n = 6$ (Heat sink HS2) in case of keeping the inlet refrigerant temperature of heat sink. Constant liquid temperature ($t_k = 45$ °C), the chip temperature ($t_{chip} = \text{variable}$) within 65 °C to 105 °C. (3) Experiment 3: Applying to $D_h = 2.98$ mm, tube quantity $n = 9$ (Mini-channel heat sink HS3) in case of keeping the inlet refrigerant temperature of heat sink. Constant liquid temperature ($t_k = 45$ °C), the chip temperature ($t_{chip} = \text{variable}$) within 65 °C to 105°C. Parameters for these three studies are summarized in Table 5.

Table 5. *Parameters for experiment cases*

Experiment (Heat sink)	Hydraulic diameter (D_h)	Tube quantity (n)	Chip temperature	Refrigerant temperature
HS1	$D_h = 10.7$ mm	1	$t_{chip} = 65 \div 105$ °C	$t_k = 45$ °C
HS2	$D_h = 4.35$ mm	6	$t_{chip} = 65 \div 105$ °C	$t_k = 45$ °C

HS3	$D_h = 2.98 \text{ mm}$	9	$t_{\text{chip}} = 65 \div 105 \text{ }^\circ\text{C}$	$t_k = 45 \text{ }^\circ\text{C}$
-----	-------------------------	---	--	-----------------------------------

The main equations in this system include the heat transfer equation, the pressure drop. The heat balance equation is applied to do analysis for heat sinks.

$$Q = Q_1 + Q_2 \quad (1)$$

Where:

Q - heat transfer rate thru heat sink, kW

Q_1 - heat transfer rate thru refrigerant fluid, kW

$$Q_1 = mc_p \Delta t, \text{ kW} \quad (2)$$

m - refrigerant mass flow rate, kg/s

c_p - specific heat at constant pressure, kJ/kgK

Δt - inlet and outlet temperature difference of refrigerant, $^\circ\text{C}$

Q_2 - heat transfer rate thru atmosphere, kW

$$Q_2 = \alpha F(t_w - t_f), \text{ kW} \quad (3)$$

α - convective heat transfer coefficient of atmosphere, kW/m²K

F - heat exchange area, m²

t_w - heat exchange surface mean temperature of heat sink, $^\circ\text{C}$

t_f - mean temperature of atmosphere, $^\circ\text{C}$

The heat transfer rate belongs to total heat transfer coefficient, heat exchange area and logarithmic mean temperature difference. This is also heat sink capacity:

$$Q = kF\Delta t_{\text{LMTD}}, \text{ kW} \quad (4)$$

Where: F - heat exchange area, m²

Δt_{LMTD} - logarithmic mean temperature difference, $^\circ\text{C}$

The heat flux is calculated by:

$$q = \frac{Q}{F}, \text{ kW/m}^2 \quad (5)$$

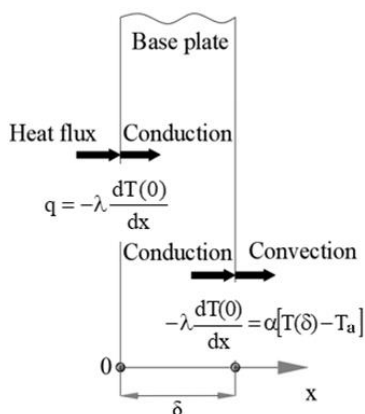
The pressure drop of heat sink is difference between the inlet pressure and the outlet pressure, [11]

$$\Delta p = p_1 - p_2 \quad (6)$$

Where: p_1 - the inlet pressure, (Pa)

p_2 - the outlet pressure, (Pa)

The boundary conditions on the base plate of the heat sink as in Fig. 8. The variation of the temperature in heat sink is given [12]. The temperatures at the inner and outer surfaces of the heat sink are determined by substituting $x = 0$ and $x = \delta$, respectively, into the relation (7):



$$T(x) = T_a + q \left(\frac{\delta - x}{\lambda} + \frac{1}{\alpha} \right) \quad (7)$$

$$T(0) = T_a + q \left(\frac{\delta}{\lambda} + \frac{1}{\alpha} \right) \quad (8)$$

$$T(\delta) = T_a + q \left(0 + \frac{1}{\alpha} \right) = T_w + \frac{q}{\alpha} \quad (9)$$

With: λ - the thermal conductivity, W/mK; q - heat flux, kW/m²; T_a - ambient temperature, K; α - convective heat transfer coefficient, kW/m²K; δ - the plate thickness (m). Where the plate thickness is from the point matches with T3 as shown in Fig. 7.

Fig. 8. The boundary conditions on the base plate of the heat sink

3. Results and discussion

3.1. The temperature profile of heat sinks with respective heater temperature

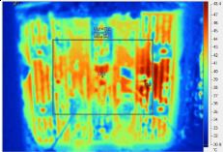
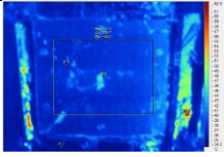
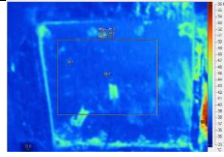
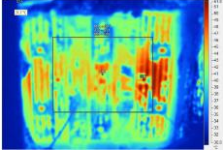
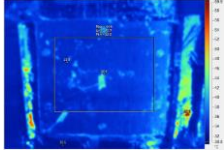
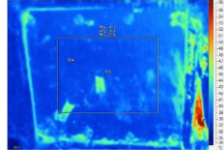
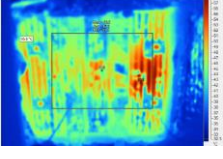
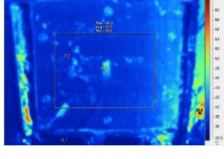
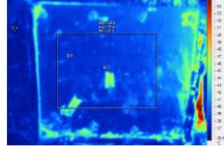
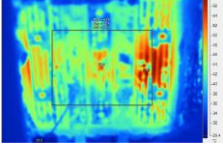
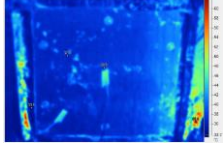
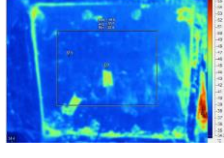
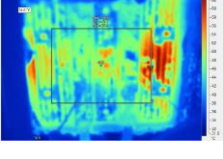
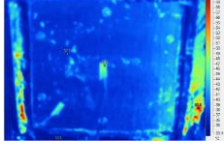
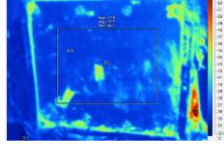
The resistor capacity was varying from 100 W to 450 W, chip temperature was varying from 65 °C to 105 °C. Three heat sinks tends to increase while increasing chip temperature. While chip temperature obtains 105 °C, the surface temperature of HS1, HS2, HS3 has temperature 49.8 °C, 47.2 °C, 48.9 °C, respectively. The surface temperature of HS1 has maximum value 49.8 °C. The surface temperature of HS2 has minimum value 47.2 °C. It has different temperature 5.2% with the surface temperature of HS1. Temperature distribution level is shown by color distribution. With HS3, the surface temperature obtains 48.9 °C, it is lower than the surface temperature of HS1 but higher than the surface temperature of HS2. Temperature distribution of HS is shown in Table 6. This shows that temperature distribution of HS2 is evenly distributed and the heat flux is higher than HS1, HS3.

3.2. Heat sink with hydraulic diameter size $D_h = 10.7$ mm, tube quantity $n = 1$

With experiment condition for this HS1, hydraulic diameter and heat sink size used for this case with $D_h = 10.7$ mm and $n = 1$, refrigerant liquid temperature and refrigerant mass flow rate were fixed at 45 °C and 0.0668 kg/s, respectively. The chip temperature was varying from 65 °C to 105 °C.

Fig. 9 shows a relationship between the chip temperature and the temperature difference of refrigerant at the condition stated above. This heat sink mean surface is calculated by average of temperature value T3, T4, T5, and T6 which measured by sensors and recorded by MX100 data acquisition unit. The temperature difference tends to increase while increasing resistor capacity from 100 W to 450 W.

Table 6. Temperature distribution of heat sinks with chip temperature from 45 °C to 105 °C

Chip temperature	Heat sinks		
	HS1	HS2	HS3
65 °C			
75 °C			
85 °C			
95 °C			
105 °C			

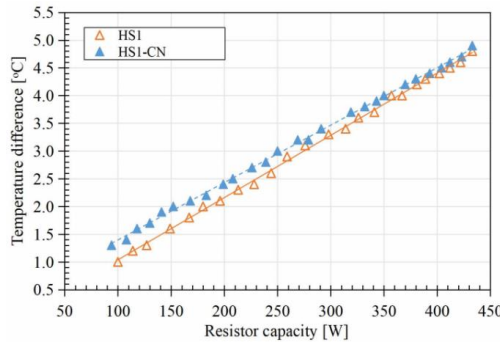


Fig. 9. Temperature difference of refrigerant fluid

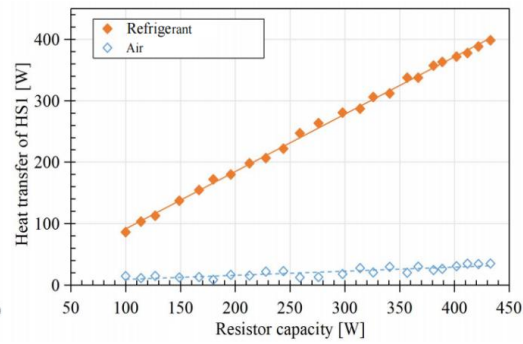


Fig. 10. The heat transfer rate

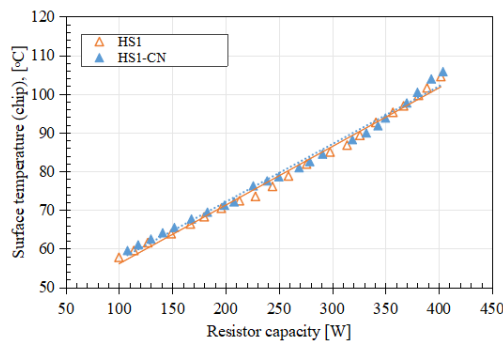


Fig. 11. The chip temperature

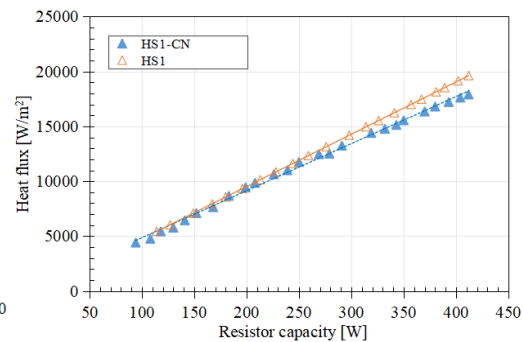


Fig. 12. The heat flux

While the chip temperature obtains 105 °C, when the temperature difference of refrigerant of HS1 which insulated (4.6 °C) higher than 15% if compared to the temperature difference of refrigerant of HS1 in case of no insulation (4.0 °C). Fig. 10 shows that resistor capacity increases, the heat transfer rate of HS1 tends to increase. While the chip temperature obtains 105 °C, the heat transfer rate of HS1 is 412 W. This is the obtained heat transfer rate because refrigerant received heat source of resistor. The heat transfer rate which convectively exchanges to air environment tends to slightly increase. While the chip temperature obtains 105 °C, the heat transfer rate of HS1 which convectively exchanges to air environment has 46 W. This shows that the heat transfer rate which convectively exchanges to air environment is equal to 11% lower than the heat transfer rate which refrigerant receives. Fig. 11 shows that the chip temperature of HS1 needs to be maintained. The chip temperature tends to increase from 65 °C to 105 °C while respectively increasing resistor capacity from 100 W to 450 W. While resistor capacity increases to 152 W, the chip temperature obtains 65 °C. While resistor capacity increases to 412 W, the chip temperature obtains 105 °C. Fig. 12 shows that while increasing resistor capacity from 100 W to 450 W leads to the heat flux increases. The respective heat flux with resistor capacity from 100 W to 412 W to obtain 65 °C and 105 °C while insulated HS1 has 5142 W/m² and 19619 W/m². The respective heat flux with resistor capacity from 100 W to 412 W to obtain 65 °C and 105 °C while HS1 is not insulated, has 4714 W/m² and 18143 W/m². This shows that the heat flux of the insulated HS1 is higher than 8.1% if compared to the heat flux of the HS1 which is not insulated.

3.3. Comparison of three heat sinks

3.3.1. Comparison of the refrigerant temperature difference and the surface temperature

Fig. 13 shows that refrigerant temperature difference tends to increase while resistor capacity increases from 100 W to 450 W with respective chip temperature obtains from 65 °C to 105 °C. While the chip temperature obtains 105 °C, maximum refrigerant temperature difference of HS1, HS2, HS3 is 4.6 °C, 4.9 °C, and 4.1 °C. This shows that refrigerant temperature difference of HS2 is higher than of HS1 (6.5%), and higher than of HS3 (19.5%). Because refrigerant temperature difference of HS2 increases, leads to the heat transfer rate of HS2 increases, and the heat flux of HS2 also respectively increases. Fig. 14 shows that while the chip temperature obtains 105 °C, outside surface temperature of

HS1, HS2, HS3 is 49.8 °C, 47.2 °C, and 48.9 °C. This results that outside surface temperature of HS2 is lower than of HS1 (5.5%), and lower than of HS3 (1.8%). Average outside surface temperature of HS1, HS2, HS3 is 47 °C, 44.3 °C, and 45.8 °C. Lowest outside surface temperature of HS1, HS2, HS3 is 42.3 °C, 39.2 °C, and 41.6 °C.

3.3.2. Comparison of the chip temperature and the heat flux

Fig. 15 shows that refrigerant temperature difference increases from 1 °C to 5 °C. This results that refrigerant temperature difference increases, the surface temperature of resistor respectively increases. The surface temperature of HS2 is lowest if compared to of HS1, of HS3. Fig.16 shows that while resistor capacity increases from 100 W to 450 W, the heat flux respectively increases. Experimental results show refrigerant temperature difference increases due to receiving heat thru refrigerant fluid from heat source of resistor, leads to the heat transfer rate increases. From study results, the heat flux of HS2 is higher than of HS1, of HS3.

3.3.3. Comparison of the heat transfer coefficient

Fig.17 shows that refrigerant temperature difference increases, leads to heat transfer coefficient increases. Result shows that heat transfer coefficient of HS2 is higher than of HS1, of HS3. Therefore, while the more resistor capacity is high, the more refrigerant temperature difference between inlet and outlet increases. From that, it leads to refrigerant temperature difference increases. Besides, heat sink HS1 has heat flux is higher than HS1 because surface area of copper tube is higher (11474 mm²), surface area of copper tube of HS1 just has 4704 mm². Because section area 89.1 mm² of HS2 is lower than of HS1 (89.9 mm²), it leads to refrigerant velocity increases. This leads to convective heat dissipation coefficient of refrigerant inside copper tube increases. From that, heat transfer coefficient increases. Experimental result as Fig. 17 is verified.

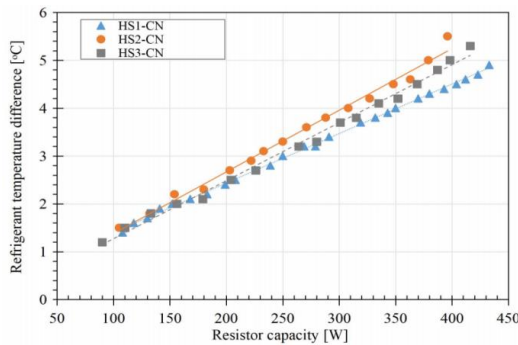


Fig. 13. Refrigerant temperature difference

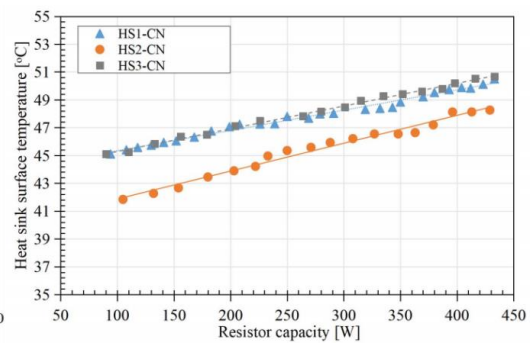


Fig. 14. Heat sink surface temperature

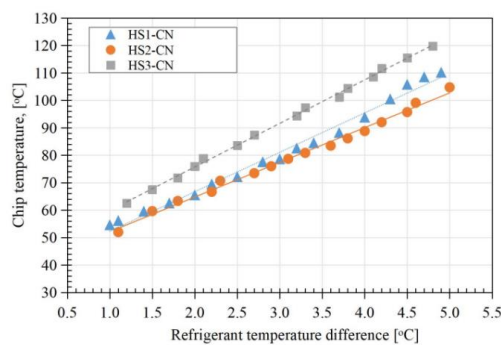


Fig. 15. Comparison of the chip temperature

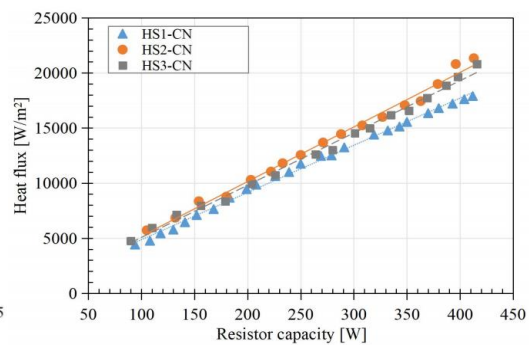


Fig. 16. Comparison of the heat flux

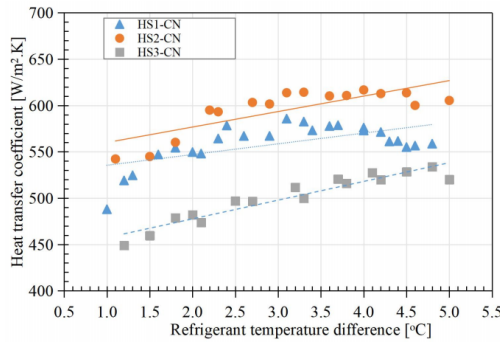


Fig. 17. Heat transfer coefficient

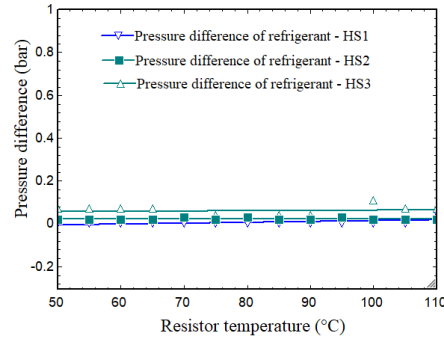


Fig. 18. Comparison of pressure difference

3.3.4. Comparison of pressure difference

While resistor capacity increases from 100 W to 450 W, the chip temperature is varying from 65 °C to 105 °C. Experimental results show that value of pressure difference is measured by digital pressure meter, does not much change as shown in Fig. 18. Pressure difference tends to horizontal line. Pressure difference of HS2 is higher than HS1 but smaller than HS3 because of hydraulic diameter size change. Hydraulic diameter D_h is smaller so pressure difference ΔP increases. In case, heat sink is heated, pressure difference of HS1, HS2, HS3 has respective value 0.01 bar, 0.02 bar, and 0.06 bar. Pressure difference tends to increase while heater temperature increases. Because while heater temperature increases, kinematic viscosity also respectively decreases.

4. Conclusion

Experiment work was done for HS1, HS2, HS3 samples. The heat transfer rate and the heat flux were determined. While increasing resistor capacity from 100 W to 450 W, the surface temperature (chip) increases from 65 °C to 105 °C. This leads the temperature difference of refrigerant fluid also increases. While the chip temperature obtains 105 °C, the maximum temperature difference of refrigerant fluid of HS1, HS2, and HS3 is 4.6 °C, 4.9 °C, and 4.1 °C, respectively. The maximum temperature difference of refrigerant fluid of HS2 is higher than of HS1 (6.5%) and of HS3 (19.5%). While the chip temperature obtains 105 °C, outside surface temperature of HS1, HS2, HS3 is 49.8 °C, 47.2 °C, and 48.9 °C. This results that outside surface temperature of HS2 is lower than of HS1 (5.5%), and lower than of HS3 (1.8%). Lowest outside surface temperature of HS1, HS2, HS3 is 42.3 °C, 39.2 °C, and 41.6 °C. The resistor capacity is at 400 W, heat flux of HS1, HS2, HS3 obtains 20047 W/m², 19294 W/m², 17712 W/m², respectively. From study results, the heat flux of HS2 is higher than of HS1 (4%), of HS3 (13%). Result shows that heat transfer coefficient of HS2 is higher than of HS1 (7%), of HS3 (18%). The heat flux of HS2 is highest if compared to of HS1, of HS3. The heat flux of HS3 is higher than of HS1. In this study, the refrigerant liquid temperature and mass flow rate are constant. The trends from experiment results show the effectiveness of increasing the heat transfer rate thru hydraulic diameter decreases, the copper tube quantity increases. This creates to increase the heat exchange surface area thru the surface area receiving the heat of refrigerant liquid. Therefore, heat sink HS2 has highest heat flux. Besides, heat transfer coefficient of HS2 is higher than of HS1, of HS3. Moreover, temperature profile of heat sinks obtained thru specialized thermal camera, demonstrated that temperature distribution of HS2 is evenly distributed on heat flux if compared to HS1 and HS3. The HS2 pressure difference of 0.02 bar is higher than HS2 having 0.01 bar. This increasingly improves for the head of compressor. Total pressure difference is still under control in range of compressor operation. This study proposed a model of the heat sink which brings the effectiveness on the heat transfer and increasing the heat flux. Based on this experiment results, it can be completely applied to VRF outdoor system to help to reduce the overheating error in VRF outdoor inverter board.

Acknowledgments

We acknowledge the support and time provided by HCMC University of Technology and Education (HCMUTE), as well as the use of facilities in this study.

Conflict of Interest

The authors declare no conflict of interest.

REFERENCES

- [1] N. Tran, Y. J. Chang, J. Teng, and R. Greif, "A study on five different channel shapes using a novel scheme for meshing and a structure of a multi-nozzle microchannel heat sink," *International Journal of Heat and Mass Transfer*, vol. 105, pp. 429-442, 2017.
- [2] F. J. Nascimento, H. Leão, and G. Ribatski, "An experimental study on flow boiling heat transfer of R134a in a microchannel-based heat sink," *Experimental thermal and fluid science*, vol. 45, pp. 117-127, 2013.
- [3] P. Thiangtham *et al.*, "An experimental study on two-phase flow patterns and heat transfer characteristics during boiling of R134a flowing through a multi-microchannel heat sink," *International Journal of Heat and Mass Transfer*, vol. 98, pp. 390-400, 2016.
- [4] N. Karwa, C. Stanley, H. Intwala, and G. Rosengarten, "Development of a low thermal resistance water jet cooled heat sink for thermoelectric refrigerators," *Applied Thermal Engineering*, vol. 111, pp. 1596-1602, 2017.
- [5] R. Zhao, Z. Wang, Y. Sun, F. Wang, and D. Huang, "Effect of the Number of Circuits on a Finned-Tube Heat Exchanger Performance and Its Improvement by a Reversely Variable Circuitry," *Applied Sciences*, vol. 12, no. 18, p. 8960, 2022.
- [6] G. Xia, J. Jiang, J. Wang, Y. Zhai, and D. Ma, "Effects of different geometric structures on fluid flow and heat transfer performance in microchannel heat sinks," *International Journal of Heat and Mass Transfer*, vol. 80, pp. 439-447, 2015.
- [7] Y. Madhour, J. Olivier, E. C. Patry, S. Paredes, B. Michel, and J. R. Thome, "Flow boiling of R134a in a multi-microchannel heat sink with hotspot heaters for energy-efficient microelectronic CPU cooling applications," *IEEE Transactions on Components, Packaging and Manufacturing Technology*, vol. 1, no. 6, pp. 873-883, 2011.
- [8] H. Mohammed, P. Gunnasegaran, and N. Shuaib, "Influence of channel shape on the thermal and hydraulic performance of microchannel heat sink," *International Communications in Heat and Mass Transfer*, vol. 38, no. 4, pp. 474-480, 2011.
- [9] K. Vafai and L. Zhu, "Analysis of two-layered micro-channel heat sink concept in electronic cooling," *International Journal of Heat and Mass Transfer*, vol. 42, no. 12, pp. 2287-2297, 1999.
- [10] M. Z. U. Khan *et al.*, "Investigation of heat transfer and pressure drop in microchannel heat sink using Al₂O₃ and ZrO₂ nanofluids," *Nanomaterials*, vol. 10, no. 9, p. 1796, 2020.
- [11] M. H. Doan, T. T. Dang and X. V. Nguyen, "The Effects of Gravity on the Pressure Drop and Heat Transfer Characteristics of Steam in Microchannels: An Experimental Study," ISSN 1996-1073, *Energies*, vol. 13, no. 14, p. 114, 2020, doi: 10.3390/en13143575.
- [12] Heat transfer, a practical approach, Yunus A. Cengel.



Le Hoai An received her B. S in Heat and Refrigeration Technology at HCMC University of Technology and Education (HCMUTE), Vietnam, in 2008. He is studying for a master's degree; Department of Thermal Engineering; Faculty of Vehicle and Energy Engineering, HCM City University of Technology and Education, Viet Nam. Currently, he is head of part of Air conditioner post sales at Samsung Vina Electronics.

Email: 2231001@student.hcmute.edu.vn. ORCID: <https://orcid.org/0009-0008-4276-3221>.



Doan Minh Hung received his B. S in Heat and Refrigeration Technology at HCMC University of Technology and Education (HCMUTE), Vietnam, in 2006. He then received his Ph.D degree at HCMC University of Technology and Education (HCMUTE), Vietnam, in 2022. His fields of interest include industrial refrigeration, heating, ventilating, and air conditioning (HVAC). Currently, he is a lecturer at the Faculty of Vehicle and Energy Engineering HCM City University of Technology and Education, Viet Nam.

Email: hungdm@hcmute.edu.vn. ORCID: <https://orcid.org/0009-0006-2632-4275>.